Chemical Geology 356 (2013) 151–159

Contents lists available at ScienceDirect

Chemical Geology

journal homepage: www.elsevier.com/locate/chemgeo

High resolution coral Cd measurements using LA-ICP-MS and ID-ICP-MS: Calibration and interpretation

Andréa G. Grottoli [a,*], Kathryn A. Matthews [b,1], James E. Palardy [b,2], William F. McDonough [c]

[a] School of Earth Science, 125 South Oval Mall, The Ohio State University, Columbus, OH, 43210, USA
[b] Department of Earth and Environmental Science, University of Pennsylvania, Philadelphia, PA 19104-6316, USA
[c] Department of Geology, University of Maryland, College Park, MD 20472, USA

ARTICLE INFO

Article history:
Received 7 January 2013
Received in revised form 15 July 2013
Accepted 13 August 2013
Available online 20 August 2013

Editor: D.B. Dingwell

Keywords:
ICP-MS
Cadmium
Cd/Ca
Coral
Seawater
Calibration

ABSTRACT

Cadmium (Cd) concentrations in coral skeleton track oceanic upwelling, which brings Cd-rich deep water to the surface. In this study we report sub-monthly measurements of $[\mathrm{Cd}]_{\mathrm{coral}}$ measured via laser ablation-inductively coupled plasma-mass spectrometry (LA-ICP-MS) in three species of coral (*Porites lobata*, *Pavona gigantea*, and *Pavona clavus*) from an upwelling site in the Gulf of Panama. Although single LA tracks in all species yielded variable results, the average of multiple tracks mirrored changes in in situ seawater Cd ($[\mathrm{Cd}]_{\mathrm{sw}}$), with an offset between peaks. In addition, $[\mathrm{Cd}]_{\mathrm{coral}}$ determined by LA-ICP-MS and isotope dilution (ID)-ICP-MS was compared in *P. clavus* and found to be highly correlated, despite consistently lower concentrations measured using the ID method. Two 5.5-month long high-resolution *P. clavus* $[\mathrm{Cd}]_{\mathrm{coral}}$ records revealed that the maximum $[\mathrm{Cd}]_{\mathrm{coral}}$ values occurred after the sea surface temperature minimum, at the same time as the seawater phosphate concentration and coral P/Ca maximum, and approximately one month before peak $[\mathrm{Cd}]_{\mathrm{sw}}$. Based on these findings we hypothesize that corals are actively taking up Cd and incorporating it into their skeleton, and that $[\mathrm{Cd}]_{\mathrm{sw}}$ only increases once Cd is no longer being rapidly removed from the water column via biological processes. After accounting for a 1-month offset between the coral and seawater [Cd] maxima, both LA- and ID-derived $[\mathrm{Cd}]_{\mathrm{coral}}$ values were significantly correlated to $[\mathrm{Cd}]_{\mathrm{sw}}$, providing a calibration for this $[\mathrm{Cd}]_{\mathrm{sw}}$ proxy in *P. clavus*. A three year high-resolution *P. clavus* LA-$[\mathrm{Cd}]_{\mathrm{coral}}$ record demonstrated the potential of $[\mathrm{Cd}]_{\mathrm{coral}}$ to generate a high-resolution $[\mathrm{Cd}]_{\mathrm{sw}}$ record. However, due to the natural variability in high-resolution LA-ICPMS $[\mathrm{Cd}]_{\mathrm{coral}}$ values within and among coral colonies, three laser tracks per colony and at least three colonies of *P. clavus* need to be analyzed to produce a reliable coral $[\mathrm{Cd}]_{\mathrm{coral}}$ record.

1. Introduction

The use of long-lived coral colonies to reconstruct paleoceanographic conditions over the past several centuries is well established. Annual bands of biogenic aragonite record environmental changes as fluctuations in both isotopic (e.g., δ^{18}O, δ^{13}C, Δ^{14}C) and elemental ratios (e.g., Sr/Ca, Ba/Ca, U/Ca) present in the skeleton [see reviews in Eakin and Grottoli, 2006; Grottoli and Eakin, 2007]. Coral Cd [reported as both Cd/Ca, and Cd concentration ($[\mathrm{Cd}]_{\mathrm{coral}}$)] appears to track oceanic upwelling (e.g., Shen et al., 1987; Linn et al., 1990; Shen and Sanford, 1990; Delaney et al., 1993; Matthews et al., 2008; Carriquiry and Villaescusa, 2010). Cadmium is bio-depleted in surface waters and more concentrated at depth, resulting in a scavenged, nutrient-type depth profile (Cullen and Maldonado, 2013). During upwelling, corals are bathed in Cd-rich water and appear to incorporate the element in proportion to the seawater concentration ($D_{\mathrm{Cd}} = (\mathrm{Cd/Ca})_{\mathrm{coral}} / (\mathrm{Cd/Ca})_{\mathrm{sw}} = 0.7\text{–}1.3$) (Shen and Sanford, 1990).

However, all $[\mathrm{Cd}]_{\mathrm{coral}}$ and/or Cd/Ca records to date have been reported at relatively low resolution (i.e., seasonal to annual), do not always capture known upwelling events, and can vary widely between species and among colonies (e.g., Delaney et al., 1993; Reuer et al., 2003; Matthews et al., 2008). For example, four *Pavona clavus* cores collected from Urvina Bay, Galápagos yielded two records with a range of 5–35 Cd/Ca (nmol mol^{-1}), while the others varied from 2 to 7 nmol mol^{-1} (Delaney et al., 1993). Low resolution (4 samples yr^{-1}) records from the eastern area of the Galápagos archipelago did capture upwelling-related seasonality (Linn et al., 1990; Shen and Sanford, 1990), but records from the western Galápagos showed minimal seasonal contrast (Delaney et al., 1993). Time series from two different species in the seasonally upwelling Cariaco Basin (Atlantic Ocean) had dissimilar trends over two decades (Reuer et al., 2003), whereas the two-decade time series from 3

---

* Corresponding author. Tel.: +1 614 292 5782.
E-mail addresses: grottoli.1@osu.edu (A.G. Grottoli), kmatthews@pewtrusts.org (K.A. Matthews), palardy@gmail.com (J.E. Palardy), mcdonoug@geol.umd.edu (W.F. McDonough).

[1] Current address: Ocean Science Division, The Pew Charitable Trusts, Washington DC 20004, USA.

[2] Current address: Environment and Resources Division, Abt Associates Inc., Bethesda, MD 20816, USA.

0009-2541/$ – see front matter © 2013 Elsevier B.V. All rights reserved.
http://dx.doi.org/10.1016/j.chemgeo.2013.08.024

coral species in the Gulf of California found that although Cd/Ca in all species varied with the El Niño Southern Oscillation (ENSO), these differences were only significant in *Pavona gigantea* (Carriquiry and Villaescusa, 2010). Finally, the presence of upwelling [as indicated by changes in sea surface temperature (SST)] coincided with significantly higher $[\mathrm{Cd}]_{\mathrm{coral}}$ in the Gulf of Panama, but there was no significant difference in the average concentration of Cd in the seawater ($[\mathrm{Cd}]_{\mathrm{sw}}$) between the upwelling and non-upwelling periods (Matthews et al., 2008). This apparent disagreement between seawater Cd, coral Cd, and SST as well as the large variance observed among time series records from different species and individuals, pose challenges to the construction and interpretation of Cd-derived paleoupwelling records.

Problems with reproducibility among colonies and species are not unique to Cd records and have been documented for Sr/Ca, Mg/Ca, U/Ca, and Ba/Ca (Hart and Cohen, 1996; Fallon et al., 2003; D. Sinclair, 2005; D.J. Sinclair, 2005). Detailed examinations of these proxies with micron-scale analytical tools, such as laser ablation-inductively coupled plasma-mass spectrometry (LA-ICP-MS), have not only generated high resolution paleoclimate records, but have shed further light on the processes that mediate proxy incorporation (D. Sinclair, 2005; D.J. Sinclair, 2005) and increased the reliability and interpretation of those proxy records. To date, similar high-resolution work with cadmium has not been done. We propose that the apparent lack of a strong relationship between $[\mathrm{Cd}]_{\mathrm{coral}}$ and upwelling or $[\mathrm{Cd}]_{\mathrm{sw}}$ may in part be an artifact of low-resolution analysis.

Coral Cd has posed a challenge to paleoceanographers due to its low concentration in coral, particularly when compared to barium (1000× more concentrated than Cd) and strontium (1,000,000× more concentrated than Cd). A more recent method using isotope dilution (ID)-ICP-MS improved the analytical detectability and precision of Cd using samples half as large as previously needed using non-ID-ICP-MS methods (Matthews et al., 2006). Unfortunately, time-intensive drilling, pre-cleaning, and matrix separation limits analytical productivity to approximately 5 samples per day thus hindering the capacity to make long $[\mathrm{Cd}]_{\mathrm{coral}}$-based paleo-reconstruction. Elemental measurements on corals by LA-ICP-MS has the advantage over ID-ICP-MS because it involves reduced sample preparation time with increased sample throughput (approximately 30 samples day^{-1}), negligible consumption of sample material, and potential for high resolution analysis (Sinclair et al., 1998). To date, LA-ICP-MS has not been used for upwelling reconstruction with $[\mathrm{Cd}]_{\mathrm{coral}}$, in part because of the challenges in making low concentration measurements (<40 ng g^{-1} at seasonally upwelling sites). Additionally, no study has yet presented concurrent seawater and coral Cd data in order to quantify upwelling influence on seawater chemistry and directly calibrate it to coral Cd.

The goals of the research presented were fourfold: 1) to survey LA-derived high-resolution (i.e., biweekly to monthly) coral Cd results from three species, 2) to compare paired high-resolution LA-ICP-MS and high-resolution high-precision ID-ICP-MS measurements in the most promising species, *P. clavus*, 3) to calibrate *P. clavus* $[\mathrm{Cd}]_{\mathrm{coral}}$ with high resolution in situ SST and $[\mathrm{Cd}]_{\mathrm{sw}}$ data, and 4) to produce a proof of concept 3-year high-resolution *P. clavus* $[\mathrm{Cd}]_{\mathrm{coral}}$ record derived from LA-ICP-MS and its accompanying predicted $[\mathrm{Cd}]_{\mathrm{sw}}$ record based on the calibration equation. As such, this study aims to determine the quality and fidelity of LA measurements of Cd in corals, and calibrate $[\mathrm{Cd}]_{\mathrm{coral}}$ to $[\mathrm{Cd}]_{\mathrm{sw}}$. Such findings would be invaluable for facilitating multi-century high-resolution (i.e., sub-monthly) $[\mathrm{Cd}]_{\mathrm{coral}}$ records in which the timing and intensity of paleoupwelling events could be accurately determined.

2. Methods

2.1. Study site and samples

The study site was located on a fringing reef on Isla Contadora (8°37′23″N; 79°02′31″W) in the Gulf of Panamá. The migration of the Intertropical Convergence Zone to the south of the gulf during the winter months brings strong northerly winds that induce upwelling in this region between January and April. During upwelling the surface ocean has lower SST, and higher sea surface salinity (SSS), Chlorophyll *a* (Chl a), and nutrient concentrations (D'Croz et al., 1991; D'Croz and Robertson, 1997). Further details on the oceanographic and reef conditions in the Gulf of Panamá are described in D'Croz and Robertson (1997) and Glynn and Mate (1997).

This study targeted *Porites lobata*, *P. clavus* and *P. gigantea* because of their local abundance, mounding morphology, and prevalence in paleoclimatic/paleoceanographic reconstruction studies. Coral fragments (5–10 cm diameter) from 1 m depth were collected in mid-January 2003, stained with Alizarin Red, then cemented to the reef at 1 m depth and allowed to grow in situ approximately 30 m from the shoreline of Playa Cacique. Fragments were stained three times over the course of a six-month calibration period (31 January 2003, 15 April 2003, 13 July 2003) (Fig. 1), bracketing the upwelling and non-upwelling periods, respectively. The stain lines had sharp upper edges clearly identifying the dates of staining and allowed for the direct comparison of specific time intervals among replicate coral fragments from the three species. This direct staining approach avoids complications associated with linking timelines to skeletal growth bands (e.g., Delaney et al., 1993) or correlation of proxy peaks/toughs (Stephans et al., 2004). Corals were harvested in February 2004, after the tissue layer had grown past the outermost stain line, thus minimizing potential contamination of the skeletal Cd by tissue Cd. Throughout the calibration

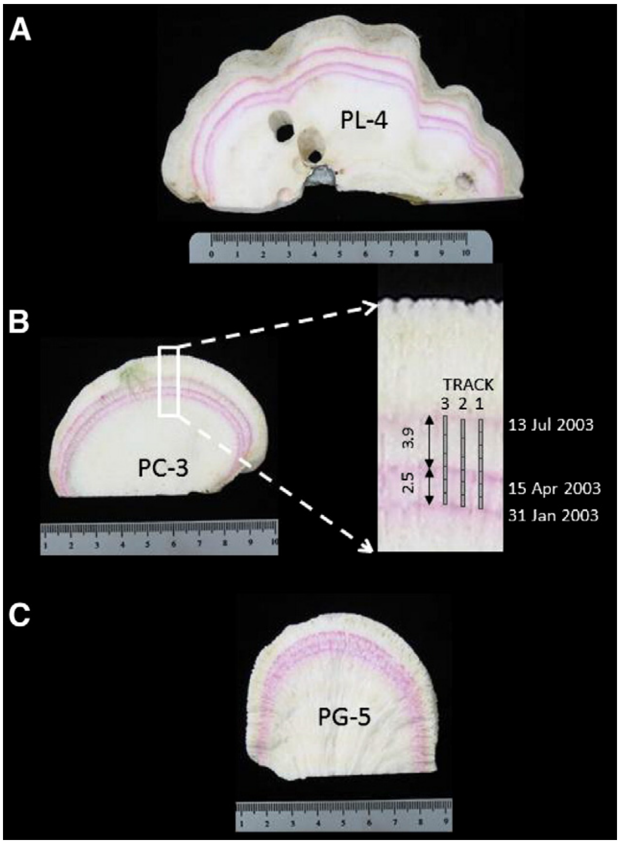

Fig. 1. Cross-section photographs of A) *Porites lobata* (PL-4), B) *Pavona clavus* (PC-3) (with inset detail of stain lines and sampling details) and C) *Pavona gigantea* (PG-5) fragments used in this study. In B) inset, dates for each stain line and the date of final collection shown on the right hand side. The measured linear skeletal growth (mm) shown between double-headed arrows on left. The three sampling tracks are shown with gray boxes indicating the area measured at each ~1 mm increment to produce the individual [Cd] values plotted with gray symbols in Fig. 2c. Ruler for scale in cm.

period, a temperature logger recorded in situ SST at a depth of 1 m every 30 min and sub-surface seawater samples were collected every three days for $[Cd]_{sw}$ analysis. Full details of the coral and water sampling methods are given in Matthews et al. (2008).

One fragment from each species was chosen for elemental analysis (*P. lobata* — PL4, *P. gigantea* — PG5; *P. clavus* — PC3) (Fig. 1). Only shallow corals (i.e., 1 m depth) were used for this study as deeper corals (i.e., 6 m) were found to have inconsistent responses in their Cd/Ca values relative to upwelling (Matthews et al., 2008). Among the 1 m depth colonies available, one fragment per species was selected based on the following four criteria: 1) a robust growth rate, 2) a well-cut slab along the growth axis, 3) the absence of bioerosion in the sampling tracks, and 4) the presence of a positive $[Cd]_{coral}$ response to upwelling at the bulk seasonal sampling scale (Matthews et al., 2008). Criteria 1–3 are consistent with strategies used in all coral-based paleoceanographic studies. Having published Cd/Ca data (criteria 4) enabled us to further refine the coral fragment selection process. Slabs 1 mm thick by 40 mm long were cut from each colony along the major axis of growth to fit the laser ablation stage, and then precleaned using methods from Matthews et al. (2006) without the reducing step prior to mounting on the stage. Due to the toxicity of the hydrazine reducing solution, the difficulty of finding airtight vessels that would hold 4-cm slabs with a minimum of airspace, and the very low likelihood of significant oxides in these young coral samples, this final reductive step was not performed on the coral slabs. Instead, a rapid initial ablation to clean the surface was performed prior to sample collection. Each slab was analyzed six times in 1-mm increments from the first stain line (31 January 2003) to the last stain line (13 July 2003) by LA-ICP-MS (see details below). The *P. clavus* fragment was also sampled from the top of the colony (14 February 2004) to ~55 mm below the growth surface. Dates were assigned for 2003–2004 assuming linear growth rates between the first and second stain lines, between the second and third stain lines, and between the last stain line and the coral growth surface. Prior to 2003, dates were assigned using skeletal banding identified on an x-radiograph of the sample and assuming linear growth between bands. Sampling resolution for all corals analyzed ranged from 1 to 2 samples/month.

In addition, the *P. clavus* fragment was analyzed using solution ID-ICP-MS at 1 mm resolution using a dental drill bit, yielding 1–2 samples/month. The drill path (1 mm wide by 0.5 mm depth) was directly adjacent to the laser tracks. Drilled samples each weighed 15–20 mg. These powdered coral samples were pre-cleaned according to the methods in Matthews et al. (2006).

2.2. Analytical methods

All analyses were carried out on an Element 2 magnetic sector field ICP-MS (Thermo Scientific Corp.) in the Plasma Laboratory at the University of Maryland. The large dynamic range of this instrument allowed for the simultaneous determination of elements with concentrations separated by 9 orders of magnitude (e.g., Ca and Cd in coral skeleton).

The LA-ICP-MS measurements were made using a frequency quintupled Nd:YAG laser operating at 213 nm (UP213, New Wave Research Corp.), coupled to the Element 2 ICP-MS, with He flushing the factory-supplied ablation cell to enhance sensitivity. Tuning and parameter adjustments (e.g., spot size, beam irradiance, repetition rate, gas flow rates) were optimized for maximum stable signal intensity and minimum oxide production. Factory-supplied software was used for the acquisition of data. The laser ablation cell was flushed with a ~1 L min^{-1} flow of He, which was supplemented with a ~0.6 L min^{-1} Ar flow at a mixing junction immediately prior to injection into the plasma torch. A typical analysis involved ~20 s of background acquisition, followed by signal acquisition via laser pulsing with a 250 μm spot size at 10 Hz for 100 s while the sample was moved at 10 μm s^{-1} along the growth axis. This resulted in a 1 mm-long sampling track. At a 1 mm-long resolution, $[Cd]_{coral}$ variability among skeletal structural elements is averaged decreasing any aliasing effects of any single structural element on the overall $[Cd]_{coral}$ signal and increasing the reproducibility of $[Cd]_{coral}$ value at a paleoceanographically relevant resolution of 2–4 weeks duration. We recognize that there are advantages and disadvantages to this type of LA sampling method. While analytical accuracy is higher with spot versus raster scans (Kroslakova and Gunther, 2007) and as spot size increases (Chen et al., 2011), spots do not evenly capture skeletal material over time. The 1-mm long raster scans are preferred because they provide biologically more meaningful representations of the elemental composition over time than spot sampling does.

For this study, the following isotopes were measured: 43Ca, 111Cd, 113Cd, and 115In. The indium isotope was included as a check for interfering isobars. A maximum of 20 samples were collected in a sequence, with the first and last two spectra acquired on NIST 612, a standard reference material. This synthetic glass from the National Institute of Standards and Technology (NIST) is a well-characterized, homogeneous silicate doped with trace elements (Pearce et al., 1997). At the time of analysis the synthetic carbonate standard, MACS-3, was not available, and NIST glasses were considered the most suitable SRMs for trace element quantification in corals (Craig et al., 2000; Fallon et al., 2003). Ca was used as the internal standard reference element for signal normalization. Tables 1 and 2 outline the operating parameters and the method file, respectively.

Raw spectral data, in ASCII format, were imported to the spreadsheet program LAMTRACE (Achterberg et al., 2001) for data reduction and quantification calculations. Signal and background selections were completed manually and data were normalized to an assumed Ca content (40.0% for the coral samples, 8.50% for the NIST standard). Absolute element concentrations were calculated based on these Ca inputs and known concentrations of elements in NIST 612.

Reporting precision, reproducibility, and accuracy is challenging for coral LA-ICP-MS results (Sinclair et al., 1998; Craig et al., 2000). The standard error of a measurement is a metric commonly used to assess precision. However this approach is only valid if the analytical signal is stable. If the signal fluctuates over time (e.g., the laser traverses a compositional gradient in the coral), then the data cannot be assumed to come from a normal sampling distribution. Thus, reporting a meaningful estimate of precision derived from a single coral LA-ICP-MS measurement is not possible. However, the reproducibility of the standards can be reported. The average relative standard deviation (rsd) from replicate analyses of NIST 612 was ±3.3% (Table 3). Another type of uncertainty is that associated with the multiple LA analyses made for each 1 mm section. The average of the standard errors of the six 1 mm analyses made along 2–3 laser tracks (see Data analysis below for details) on each coral specimen were ±2.7, 1.9 and 1.1 ng g^{-1} for *P. lobata*, *P. gigantea*, and *P. clavus*, respectively.

The full analytical procedure for the ID-ICP-MS analyses is detailed in Matthews et al. (2006). Briefly, the pre-cleaned samples were spiked with a 113Cd solution, dissolved and passed through an ion exchange resin to remove extraneous total dissolved solids. The Cd-bearing

Table 1
LA-ICP-MS configurations.

Parameter	Setting
ICP-MS model	Element 2
Laser model	New Wave UP213 nm; solid state Nd:YAG crystal with 3 harmonic generators
Ablation gas mix	He (cell only), Ar
Final beam size	250 μm spot
Laser fluence	1.85–3.10 J/cm^2
Ablation rate	10 Hz
Laser energy	Standard: 45%; Sample: 55%
Scan speed	10 mm/s

Table 2
Method parameters for elements reported. All isotopes were monitored in dynamic magnet jump and E-scan mode with 1 sample per peak, and 260 runs and 1 pass, for a sample time of 2:01 min:s. Mass resolution set at 300.

Isotope	Magnet mass	Settling time (s)	Sample time (s)	Detection mode
^{43}Ca	42.96	0.11	0.005	Analog
^{111}Cd	112.9	0.041	0.01	Both
^{113}Cd	112.9	0.001	0.01	Both

elutant was then analyzed using an Aridus dry desolvator (CETAC Technologies) for introduction to the ICP-MS. The rsd of repeated measurements of an internal coral standard using this technique was ±2.2% (n = 12).

$[\mathrm{Cd}]_{\mathrm{sw}}$ was determined using the method described in Field et al. (1999). Every two seawater samples were combined prior to analysis to create an approximately weekly resolution. A direct, ten-fold dilution of each filtered, acidified seawater sample was introduced to the ICP-MS using dry desolvation. The Gulf of Panamá samples and the CASS-4 seawater standard (National Research Council, Canada) were determined by normalized standard addition. Repeated measurements of the CASS-4 standard yielded an rsd of ±2.2% (n = 10).

2.3. Satellite data

Satellite SST and Chl a data from 2001 to 2004 were collected for the Gulf of Panamá (8°N–9°N; 79.5°W–78.5°W). Temperature data are NOAA/NCEP weekly SST fields (Reynolds and Smith, 1994) from the NOMADS data server (http://nomads.ncdc.noaa.gov). Monthly Chl a data used in this study were acquired from SeaWiFS using the GES–DISC Interactive Online Visualization ANd aNalysis Infrastructure (GIOVANNI) as part of the NASA's Goddard Earth Sciences (GES) Data and Information Services Center (DISC).

2.4. Data analysis

Two to three parallel laser tracks, separated by no more than 1 mm, were traced for each coral fragment (Fig. 1B). Each track was composed of several mm-long sampling segments that were each measured six times each and averaged to produce a single value for each mm segment along each track. The total number of mm-long segments for each fragment was not always identical, as some fragments grew faster than others. Therefore, linear interpolation was used to regrid the measurements of each track to a common interval assuming constant growth rates between the stain lines. The $[\mathrm{Cd}]_{\mathrm{coral}}$ values of each track were then regridded to regular monthly intervals and averaged for each coral fragment to facilitate comparisons with the monthly ID-ICP-MS values from the same fragment.

Major-axis regression assessed the relationship between the monthly regridded-average $[\mathrm{Cd}]_{\mathrm{coral}}$ values measured using LA-ICP-MS and the parallel ID-ICP-MS values for the following reasons: 1) there is uncertainty in both data sets, and 2) both variables are measured on the same scale and with the same units (Legendre and Legendre, 1998). For the same reasons, major-axis regression was used to assess the relationship between average-regridded $[\mathrm{Cd}]_{\mathrm{coral}}$ and $[\mathrm{Cd}]_{\mathrm{sw}}$ and the relationship between the 1-month-adjusted average-regridded $[\mathrm{Cd}]_{\mathrm{coral}}$ and $[\mathrm{Cd}]_{\mathrm{sw}}$ (i.e., February $[\mathrm{Cd}]_{\mathrm{coral}}$ values with March $[\mathrm{Cd}]_{\mathrm{sw}}$).

Ordinary least-squares regression was used to assess the relationship between the average-regridded $[\mathrm{Cd}]_{\mathrm{coral}}$ and SST, and between the 1-month-adjusted average-regridded $[\mathrm{Cd}]_{\mathrm{coral}}$ and SST. Statistical analyses were generated using the lmodel2 package in R (Legendre, 2011) and JMP IN software (Version 4.0.3 SAS Institute Inc.) *P*-levels ≤0.05 were considered significant. In addition, the high-resolution in situ $[\mathrm{Cd}]_{\mathrm{coral}}$ and $[\mathrm{Cd}]_{\mathrm{sw}}$ values were used to calculate the distribution coefficient of Cd in coral skeletons [D_{Cd} where $D = (\mathrm{metal/Ca})_{\mathrm{coral}} / (\mathrm{metal/Ca})_{\mathrm{sw}}$] to infer controls over precipitation of the cation in the aragonite skeleton.

3. Results

Parallel laser tracks of LA-ICP-MS-derived $[\mathrm{Cd}]_{\mathrm{coral}}$ in *P. lobata*, *P. gigantea* and *P. clavus* spanning the 6-month period of 31 January 2003 to 13 July 2003 showed generally higher values during upwelling than during non-upwelling (Fig. 2). Of the three species, the individual laser track profiles in *P. lobata* differed the most from each other (Fig. 2A). Track 2 had higher average values than Track 1 (28 ng g^{-1} vs. 23 ng g^{-1}) and a greater difference between mean upwelling and non-upwelling values (6.6 ng g^{-1} vs. 1.3 ng g^{-1}). In contrast, *P. gigantea* and *P. clavus* sampling track profiles (Fig. 2B and C) were similar with low initial concentrations, an average $[\mathrm{Cd}]_{\mathrm{coral}}$ peak of ~28 ng g^{-1} in the middle to latter portion of the upwelling interval, and lower and less variable average values of ~23 ng g^{-1} during non-upwelling. Furthermore, *P. clavus* LA-ICP-MS and ID-ICP-MS $[\mathrm{Cd}]_{\mathrm{coral}}$ values were highly correlated (Fig. 3).

During this same six-month period, SST was low and variable during upwelling with average temperatures of 24.8 °C (31 January–15 April 2003) followed by constant and warm SSTs averaging 28.3 °C (15 April–13 July 2003) (Fig. 4A). This SST range was a typical for the Gulf of Panamá during non-El Niño years (D'Croz et al., 1991; D'Croz and Robertson, 1997).

$[\mathrm{Cd}]_{\mathrm{sw}}$ also exhibited a clear response to upwelling conditions. $[\mathrm{Cd}]_{\mathrm{sw}}$ increased throughout the upwelling interval to a maximum value of 44 pg g^{-1}, then gradually decreased over the non-upwelling interval (Fig. 4A). Lastly, initial $[\mathrm{Cd}]_{\mathrm{coral}}$ values were low during initial upwelling, peaked in early April, and gradually decreased over the following two months (Fig. 4B). However, peak $[\mathrm{Cd}]_{\mathrm{coral}}$ values preceded peak $[\mathrm{Cd}]_{\mathrm{sw}}$ by approximately one month. In addition, absolute $[\mathrm{Cd}]_{\mathrm{coral}}$ values were lower by an average of 3.9 ng g^{-1} when measured via ID-ICP-MS compared to LA-ICP-MS, revealing a bias between these methods (Fig. 4B).

$[\mathrm{Cd}]_{\mathrm{coral}}$ was not significantly correlated to either SST or $[\mathrm{Cd}]_{\mathrm{sw}}$ (Table 4, Fig. 5A). When $[\mathrm{Cd}]_{\mathrm{coral}}$ was adjusted by one month (i.e., to align that peak with the later $[\mathrm{Cd}]_{\mathrm{sw}}$ peak), the regression of both LA-derived and ID-derived $[\mathrm{Cd}]_{\mathrm{coral}}$ versus $[\mathrm{Cd}]_{\mathrm{sw}}$ was statistically significant and accounted for 82–87% of the variability (Table 4, Fig. 5B). These regressions define the calibration between $[\mathrm{Cd}]_{\mathrm{coral}}$ and $[\mathrm{Cd}]_{\mathrm{sw}}$ from a single *P. clavus* colony and specify that for a given $[\mathrm{Cd}]_{\mathrm{coral}}$ value measured in month *t*, the predicted $[\mathrm{Cd}]_{\mathrm{cw}}$ value for the following month $(t + 1)$ is

$$\text{LA-}[\mathrm{Cd}]_{\mathrm{coral},t} = \left(0.63\ [\mathrm{Cd}]_{\mathrm{sw},t+1}\right) + 3.61 \tag{1}$$

$$\text{ID}-[\mathrm{CD}]_{\mathrm{coral},t} = \left(0.86\ [\mathrm{Cd}]_{\mathrm{sw},t+1}\right) - 7.59 \tag{2}$$

Table 3
NIST 612 results. The detection limit was defined as 3 times the lower limit of detection. The relative standard deviation (rsd) was calculated from the sd of the four NIST 612 Cd measurements made during every sample sequence. The precision reported here is the lower limit on the actual measurement error.

Date (2006)	Detection limit (ppm)	rsd (%)
11 Aug	0.0008	2.1
11 Aug	0.0005	3.6
11 Aug	0.0008	3
20 Sept	0.0005	2.5
20 Sept	0.0006	3.6
28 Sept	0.0006	5.7
06 Oct	0.0005	3.3
06 Oct	0.0005	3.5
06 Oct	0.0004	2.5
Average	0.0006	3.3

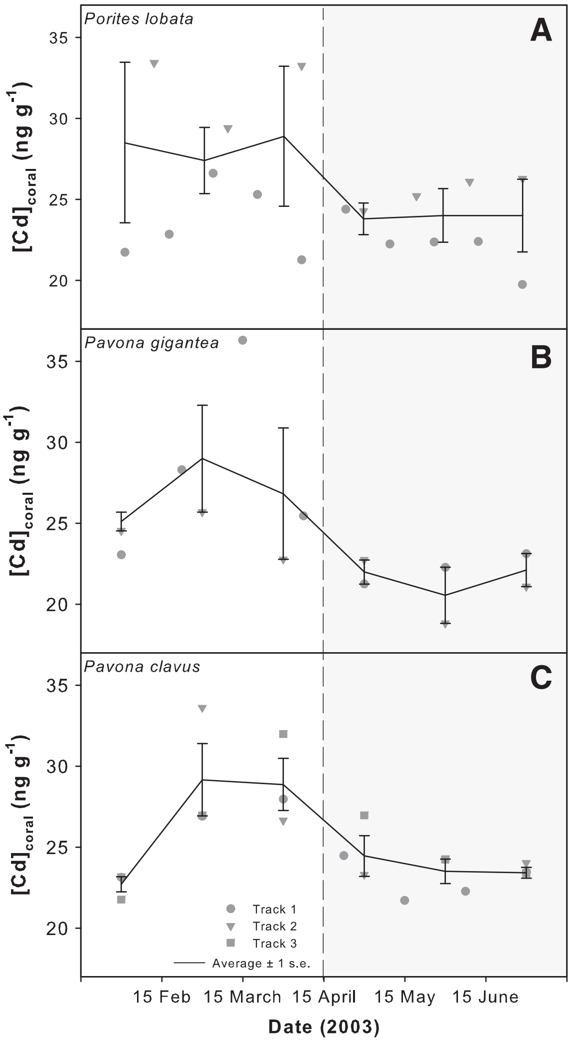

Fig. 2. Coral [Cd] via LA-ICP-MS in three species of corals. LA-ICP-MS derived $[\text{Cd}]_{\text{coral}}$ from parallel tracks of A) *Porites lobata*, B) *Pavona gigantea*, and C) *Pavona clavus* colonies spanning the upwelling (white background) and non-upwelling (gray background) seasons. Stain lines represented by vertical lines (31 January = left-hand y-axis, 15 April = vertical dashed line, 13 July = right-hand y-axis).

where LA-$[\text{Cd}]_{\text{coral}}$ and ID-$[\text{Cd}]_{\text{coral}}$ are in ng g^{-1} and $[\text{Cd}]_{\text{sw}}$ is in pg g^{-1}. These equations can be rearranged so that predicted $[\text{Cd}]_{\text{sw}}$ values can be reconstructed from $[\text{Cd}]_{\text{coral}}$ values as follows:

$$\text{Predicted } [\text{Cd}]_{\text{SW},t+1} = \frac{\text{LA-}[\text{Cd}]_{\text{coral},t} - 3.61}{0.63} \tag{3}$$

$$\text{Predicted } [\text{Cd}]_{\text{SW},t+1} = \frac{\text{ID–}[\text{Cd}]_{\text{Coral},t} + 7.59}{0.86}. \tag{4}$$

LA-ICP-MS measurements of a 55 mm-long section of the *P. clavus* fragment produced a 3-year $[\text{Cd}]_{\text{coral}}$ record with an average sampling resolution of 2.8 weeks/sample. This record exhibited clear seasonality, with $[\text{Cd}]_{\text{coral}}$ peaks in early 2001, 2002, and 2003 that generally followed troughs in SST and peaks in Chl *a* by ~1 month (Fig. 6). Peak $[\text{Cd}]_{\text{coral}}$ from 2003 was more enriched in Cd compared to the peak values from the 2001 and 2002 upwelling seasons (20–30 ng g^{-1} vs. 15–20 ng g^{-1}). Upwelling intensity as gauged by satellite SST and Chl *a* did not show a similar increase in magnitude in 2003 compared to previous years, although it should be noted that the satellite SST minimum (~26 °C) was higher than the in situ 1 m depth temperature logger by 4 °C (~22 °C). The predicted $[\text{Cd}]_{\text{sw}}$ values for the entire 3-year record mirrored $[\text{Cd}]_{\text{coral}}$ with a 1-month offset (Fig. 6C).

3.1. Distribution coefficient of Cd in coral skeleton (D_{Cd})

D_{Cd} for *P. clavus* in the Gulf of Panama was 1.7 and 1.3 when calculated with LA- and ID-derived $[\text{Cd}]_{\text{coral}}$ data, respectively, and where $[\text{Cd}]_{\text{sw}}$ was measured in situ with an assumed concentrations of 10.27 mmol Ca/kg (Horibe et al., 1974). These findings are generally consistent with previous estimates of $D_{\text{Cd}} \approx 1$ (Shen et al., 1987; Shen and Sanford, 1990), indicating a dominant kinetic control on metal incorporation. However, the higher-resolution data in this study allowed for a more precise calculation of D that indicates a slight preferential uptake of Cd into the coral skeleton relative to its abundance in seawater.

4. Discussion

4.1. Within and among species variability in LA-ICP-MS derived $[\text{Cd}]_{\text{coral}}$

The natural variability in LA-derived $[\text{Cd}]_{\text{coral}}$ within and among *P. lobata*, *P. gigantea*, and *P. clavus* was evaluated. The range of LA-$[\text{Cd}]_{\text{coral}}$ values in *P. lobata* was much lower (22 to 34 ng g^{-1}; Fig. 2A) than previously observed in a coastal *P. lobata* colony influenced by terrestrial runoff (<10 ng g^{-1} to 70 ng g^{-1}; Alibert et al., 2003). At the same time the variability between the Track 1 and 2 profiles (Fig. 2A) was the greatest compared to both Pavonid corals (Fig. 2B, C). The cause for the high within-colony variability might be Cd compositional differences among skeletal elements and/or the inability of the sampling spot size to capture the complete environmental signature. Although Allison and Finch (2004) found significant differences in Sr/Ca among skeletal elements of *P. lobata*, it is not likely the case in this instance. The spot size used here was 25 times larger than in Allison and Finch (2004) and covered multiple skeletal elements of the fine-structured *P. lobata* at a time. Thus, one or two laser tracks are insufficient in *P. lobata* to give a representative LA-$[\text{Cd}]_{\text{coral}}$ record using our methodology.

In *P. gigantea*, the results from Track 1 more closely resembled the range observed in bulk sample data reported in Matthews et al. (2008), while Track 2 displayed a more muted response (Fig. 2B). Given the laser spot size (250 μm) and the coarse skeletal structure of *P. gigantea*, it was difficult to encompass multiple structural elements increasing the likelihood that skeletal heterogeneity may have affected the results. In the future, a larger spot size is recommended [as suggested in Sinclair et al., 1998 and Fallon et al., 2003] for this species.

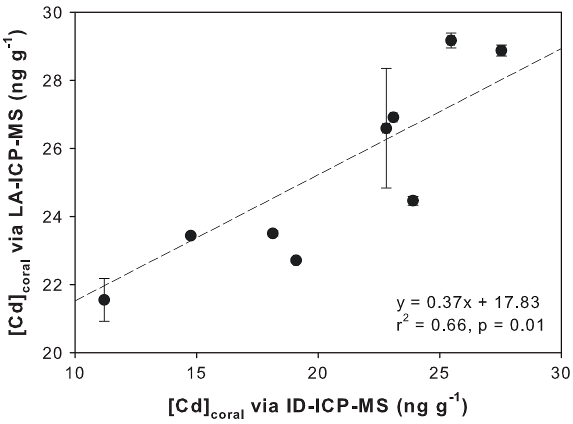

Fig. 3. Coral [Cd] by LA-ICP-MS versus ID-ICP-MS. Major axis regression of *Pavona clavus* $[\text{Cd}]_{\text{coral}}$ by LA-ICP-MS (±1SE of the parallel laser tracks) versus paired samples by ID-ICP-MS (±2.2% rsd; errors not visible because they are smaller than the plotted symbols).

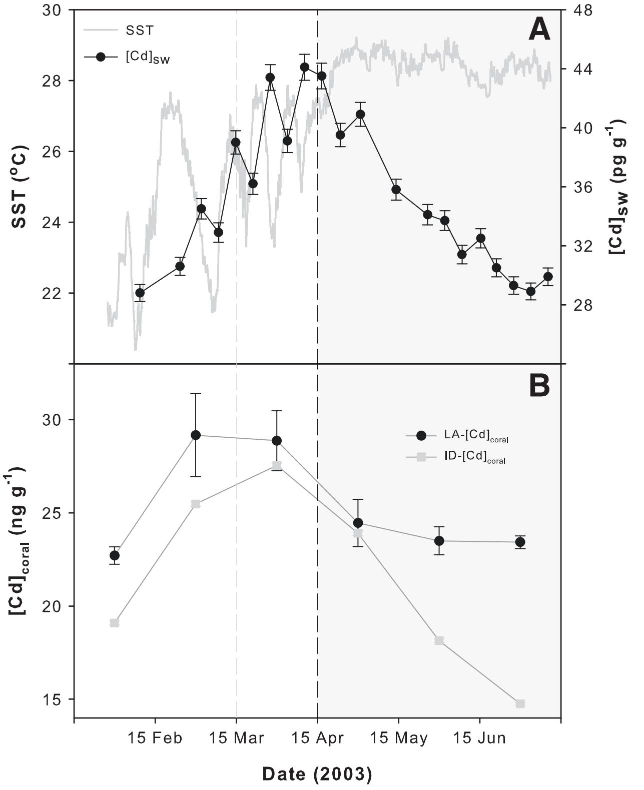

Fig. 4. Temperature, seawater [Cd], and coral [Cd] records. A) In situ sea surface temperature (SST, measured twice hourly and smoothed with a 48-point running mean) and seawater Cd ($[Cd]_{sw}$ ± 1 rsd) from Isla Contadora, Gulf of Panamá and B) *Pavona clavus* coral Cd derived via LA-ICP-MS (average LA-$[Cd]_{coral}$ ± 1 SE from Fig. 2C) and ID-ICP-MS (ID-$[Cd]_{coral,}$ ± 2.2% rsd) spanning the upwelling (white background) and non-upwelling (gray background) seasons. Stain lines represented by black vertical lines (31 January = left-hand y-axis, 15 April = black dashed line, 13 July = right-hand y-axis). Vertical gray dashed line = peak $[Cd]_{coral}$ on 15 March. Seawater $[PO_4]$ from LaVigne et al. (2010).

In *P. clavus*, reproducibility among the three laser tracks was the strongest (Fig. 2C). This species has a much smaller polyp size and finer skeletal structure than *P. gigantea*, which would have enabled multiple skeletal elements to be simultaneously ablated by the laser and may help to account for the stronger reproducibility among laser tracks in *P. clavus* compared to *P. gigantea*.

Overall, these data highlight intra-colony and species-specific variability in LA-$[Cd]_{coral}$ values. While, coral paleoclimate records derived using single LA tracks are common for many elemental proxies (e.g., Sinclair et al., 1998; McCulloch et al., 2003) where repeated measurements of the minor (e.g., Sr, Mg) and the more concentrated trace (e.g., Ba, U) elements along parallel tracks give a reproducibility of <5% (Fallon et al., 1999, 2002), LA-derived $[Cd]_{coral}$ measurements in this study do not (Fig. 2). Measurable differences between 2 and 3 adjacent parallel tracks (Fig. 2) suggest that the arbitrary choice of laser track could yield a different "environmental" history than that from a neighboring track. As such, the average of at least 3 laser tracks is recommended to obtain a representative $[Cd]_{coral}$ record. This is in addition to the use of at least 3 replicate coral fragments recommended in Matthews et al. (2008), bringing the total number of LA-ICP-MS tracks necessary for an accurate reconstruction to nine.

Interestingly, skeletal growth and SST do not appear to have a detectable effect on $[Cd]_{coral}$ in this study for two reasons. First, corals calcified throughout the entire study period. As was demonstrated with Sr (Fallon et al., 1999), only when calcification ceases might the incorporation of Cd into the skeleton be affected. Second, $[Cd]_{coral}$ does not correlate with maximum linear skeletal extension, $\delta^{13}C$, or $\delta^{18}O$ (Matthews et al., 2008) — geochemical tracers that are typically sensitive to calcification and/or temperature (McConnaughey, 1989; Eakin and Grottoli, 2006). Thus, $[Cd]_{coral}$ is independent of skeletal growth rates and SSTs observed in this study.

Of the three species surveyed in this study, *P. clavus* yielded the highest reproducibility among $[Cd]_{coral}$ tracks and is therefore most suitable for high-resolution LA-$[Cd]_{coral}$ paleoceanographic study. This is fortuitous as *P. clavus* is abundant in the eastern tropical Pacific (Glynn and Ault, 2000) where upwelling is common and is already the species most frequently used for coral Cd measurements (Shen et al., 1987; Linn et al., 1990; Shen and Sanford, 1990; Shen et al., 1992; Delaney et al., 1993; Carriquiry and Villaescusa, 2010) and eastern Pacific paleoceanographic studies (e.g., Wellington and Dunbar, 1995).

4.2. Laser ablation vs. isotope dilution

In *P. lobata*, average LA-derived $[Cd]_{coral}$ values during upwelling and non-upwelling periods were an order of magnitude higher than the bulk values for this same coral measured via ID-ICP-MS (Table 5). Average *P. gigantea* LA-derived $[Cd]_{coral}$ values were 15% higher during upwelling and 45% higher during non-upwelling than those made on bulk skeletal samples via ID (Table 5). And, average LA-derived $[Cd]_{coral}$ values in *P. clavus* were ~12% higher during the upwelling and ~20–60% higher during the non-upwelling seasons than average high-resolution ID-$[Cd]_{coral}$ values (Table 5, Fig. 2), and bulk skeletal samples of the same corals via ID (Table 5). Thus, LA-ICP-MS may overvalue and/or ID-ICP-MS may undervalue $[Cd]_{coral}$, particularly at low concentrations, resulting in a constricted LA-$[Cd]_{coral}$ range compared to ID-$[Cd]_{coral}$.

The underlying reasons for the offset between LA- and ID-derived $[Cd]_{coral}$ values could be due to one or more of the following: 1) LA was consistently unable to measure the lowest Cd concentrations, 2) the finest particles produced from milling during the sample preparation for ID analysis preferentially incorporated Cd relative to that found in larger particles such that the loss of fine particles during ID pre-cleaning, sample transfer, and solution aspiration steps resulted in an underestimation of $[Cd]_{coral}$ via ID-ICP-MS, or 3) accuracy is lower in LA-ICP-MS analysis compared to ID-ICP-MS. We know that the detection limit was not challenged during LA analyses (Table 3), thus the disparity between LA and ID values was not likely due to an inability to measure Cd at low concentrations. The bias between LA and ID-derived $[Cd]_{coral}$ values detected in the finer-structured *P. lobata* but not in the skeletally more robust Pavonids which suffered less sample loss during the cleaning process (Matthews et al., 2008) (Table 5), is consistent with the hypothesis that Cd concentrations were higher in the finest particles. However, this possibility would also necessitate that certain micro-skeletal structural elements were more prone to producing fine particles when ground during sample preparation than other micro-skeletal elements. While possible, it seems unlikely that it could account for all of the bias observed. However, ID analyses are assumed to be inherently more accurate because of the multiple checks one can cross calibrate with this method, whereas the equivalent

Table 4
Regression results of *Pavona clavus* skeletal Cd concentration ($[Cd]_{coral}$; ng g^{-1}) measured by laser ablation inductively coupled plasma mass spectrometry (LA-ICP-MS) (LA-$[Cd]_{coral}$) and isotope dilution ICP-MS (ID-$[Cd]_{coral}$) versus sea surface temperature (SST, °C) and seawater Cd concentrations ($[Cd]_{sw}$; pg g^{-1}). Bolded equations are statistically significant at $p \leq 0.05$. Adj = 1-month adjusted.

Regression		Equation	r^2	p-Value
y	x			
LA-$[Cd]_{coral}$	**ID-$[Cd]_{coral}$**	$\mathbf{y = 0.37x + 17.8}$	**0.66**	**0.01**
LA-$[Cd]_{coral}$	SST	$y = -0.21x + 30.9$	0.03	0.73
ID-$[Cd]_{coral}$	SST	$y = -0.47x + 33.9$	0.06	0.64
LA-$[Cd]_{coral}$	$[Cd]_{sw}$	$y = 0.12x + 21.8$	0.01	0.37
ID-$[Cd]_{coral}$	$[Cd]_{sw}$	$y = 1.23x - 21.6$	0.38	0.10
adj LA-$[Cd]_{coral}$	**$[Cd]_{sw}$**	$\mathbf{y = 0.63x - 3.61}$	**0.82**	**0.05**
adj ID-$[Cd]_{coral}$	**$[Cd]_{sw}$**	$\mathbf{y = 0.86x - 7.6}$	**0.87**	**0.01**

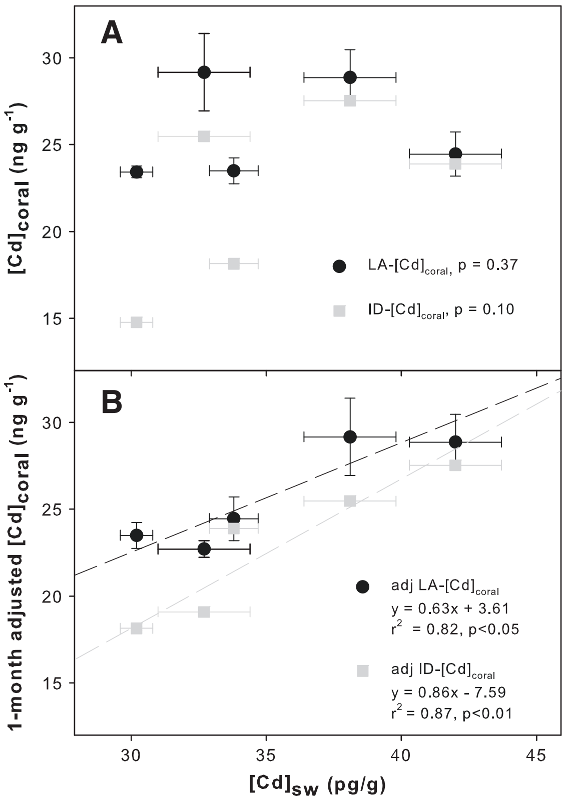

Fig. 5. Coral [Cd] versus seawater [Cd]. A) *Pavona clavus* skeletal Cd via LA (LA-$[\mathrm{Cd}]_{\mathrm{coral}}$) and ID (ID-$[\mathrm{Cd}]_{\mathrm{coral}}$) ICP-MS versus seawater Cd concentrations ($[\mathrm{Cd}]_{\mathrm{sw}}$). B) Major axis regression of one-month adjusted *P. clavus* $[\mathrm{Cd}]_{\mathrm{coral}}$ values versus $[\mathrm{Cd}]_{\mathrm{sw}}$. $[\mathrm{Cd}]_{\mathrm{sw}}$ average and SE values computed from all measurements taken during each 1 month time period. Average and SE values for $[\mathrm{Cd}]_{\mathrm{coral}}$ via LA and ID are as described for Fig. 4B. adj = 1-month adjusted.

calibrations are not available for LA-based analyses given limited mass of material interrogated during this method. Therefore, the offset between LA and ID measurements probably has more to do with accuracy of each analytical method than anything else.

Despite the bias between LA- and ID-derived $[\mathrm{Cd}]_{\mathrm{coral}}$, the measurements made on paired samples of *P. clavus* using both methods were significantly correlated (Fig. 3) indicating that LA-derived Cd measurements have the potential to generate paleoceanographically useful Cd records at very high resolution. These results agree with existing comparisons between LA and standard solution-ICP-MS for Mg, Ba, U and rare earth elements (Fallon et al., 1999; Wyndham et al., 2004). For example, a comparison of $[\mathrm{Ba}]_{\mathrm{coral}}$ records found a similar offset with LA-derived concentrations being higher than the solution-based ones (Wyndham et al., 2004). Since the offset is not unique to Cd, it suggests that there is a systematic difference between ID vs LA-derived elemental values, independent of the element measured, the cleaning methods or standards used. Nevertheless, further refinement of the LA method coupled with reduction in sample loss during pre-cleaning for ID analyses could help to improve the agreement between these two techniques.

4.3. Calibration of P. clavus $[\mathrm{Cd}]_{\mathrm{coral}}$

This study showed that while $[\mathrm{Cd}]_{\mathrm{coral}}$, $[\mathrm{Cd}]_{\mathrm{sw}}$, and SST were all sensitive to upwelling, the timing of the maximum expression of the upwelling effect on each variable was not synchronous and thus influenced the $[\mathrm{Cd}]_{\mathrm{coral}}$ versus $[\mathrm{Cd}]_{\mathrm{sw}}$ calibration. Although SST was already low at the start of the sampling period (31 January), $[\mathrm{Cd}]_{\mathrm{sw}}$ did not reach its maximum until ~15 April. The lag between minimum SST and maximum $[\mathrm{Cd}]_{\mathrm{sw}}$ suggests that dissolved Cd was rapidly consumed during the planktonic bloom triggered by the upwelling, immediately scoured from the surface waters, then returned to the water column later as the bloom began to decay and the living biota were under C-replete conditions. A similar scouring mechanism for Ba and Cd depletion in surface waters during upwelling was also hypothesized by Lea et al. (1989). With the cessation of cold-water pulses in mid-April, SST plateaued and $[\mathrm{Cd}]_{\mathrm{sw}}$ decreased gradually, most likely due to biological activity, until reaching a post-upwelling low in late June (Fig. 4A). Thus, while $[\mathrm{Cd}]_{\mathrm{sw}}$ and SST are tightly coupled, they are not perfectly synchronous — the $[\mathrm{Cd}]_{\mathrm{sw}}$ maximum *lags* the average SST seasonal minimum by ~2 months (Fig. 4A).

Comparison of SST and $[\mathrm{Cd}]_{\mathrm{sw}}$ with *P. clavus* $[\mathrm{Cd}]_{\mathrm{coral}}$ revealed that the $[\mathrm{Cd}]_{\mathrm{coral}}$ maximum *lagged* the SST minimum by 1–2 months, and that the $[\mathrm{Cd}]_{\mathrm{coral}}$ maximum *led* the $[\mathrm{Cd}]_{\mathrm{sw}}$ maximum by ~1 month (Table 4; Figs. 4, 5B). Given the well-constrained time intervals for the coral fragment via staining and the high resolution SST and $[\mathrm{Cd}]_{\mathrm{sw}}$ measurements, it is clear that peak $[\mathrm{Cd}]_{\mathrm{coral}}$ values are slightly offset from the more commonly used proxies for upwelling such as SST via $\delta^{18}\mathrm{O}$ and Sr/Ca (e.g., Dunbar et al., 1994; Wellington and Dunbar, 1995). Even if previously published Cd records (e.g., Shen and Sanford, 1990; Delaney et al., 1993; Reuer et al., 2003) with a resolution ≥3 months/sample had a concurrent $[\mathrm{Cd}]_{\mathrm{sw}}$ time series, this ~1 month lag between coral and seawater would not have been detectable at that resolution. Consistent with this study, upwelling events preceded coral Ba/Ca maxima (another upwelling proxy) by ~2 months in Shirigai Bay, Japan (Fallon et al., 1999).

Furthermore, the one-month offset in maximum coral and seawater [Cd] may be a result of the mechanism of Cd incorporation by the coral animal and/or the calcification process. First, the rapid, active uptake of dissolved $[\mathrm{Cd}]_{\mathrm{sw}}$ by plankton and coral early in the upwelling process could produce such an offset. This would be consistent with a low initial $[\mathrm{Cd}]_{\mathrm{sw}}$ during upwelling, and the occurrence of peak skeletal $[\mathrm{Cd}]_{\mathrm{coral}}$ before peak $[\mathrm{Cd}]_{\mathrm{sw}}$. Indeed, since corals can be active heterotrophs of plankton (Palardy et al., 2005; Grottoli et al., 2006; Palardy et al., 2006, 2008), such uptake is a viable mechanism for the incorporation

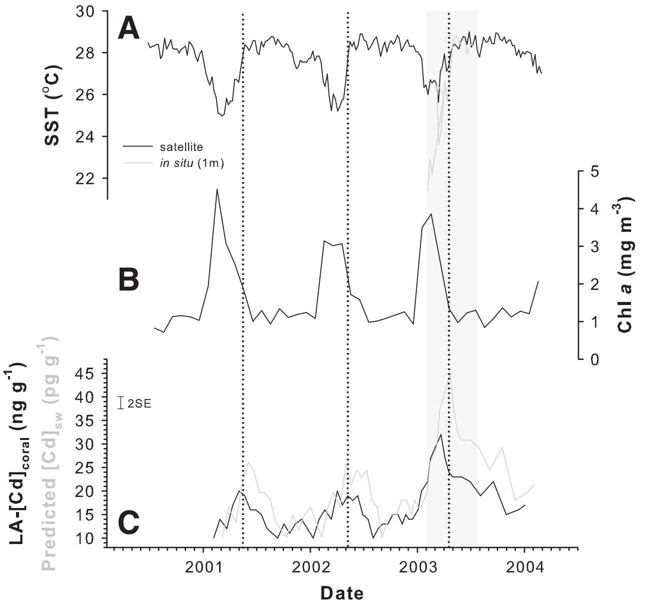

Fig. 6. Three-year, high-resolution temperature, chlorophyll *a*, coral [Cd], and predicted seawater [Cd]. A) Weekly mean sea surface temperature (SST) (Satellite data from NOAA/NCEP weekly SST fields (Reynolds and Smith, 1994); in situ SST record from Fig. 4A). B) Monthly mean chlorophyll-*a* (Chl a) concentrations (SeaWiFS). C) Sub-monthly measured *Pavona clavus* coral Cd concentrations via LA-ICP-MS (LA-$[\mathrm{Cd}]_{\mathrm{coral}}$ ± 1.1 ng g^{-1} (±1SE)) and predicted seawater Cd concentrations ($[\mathrm{Cd}]_{\mathrm{sw}}$) derived from Eq. (1). The vertical shaded area represents the January–July 2003 study period where the edges of correspond to the 31 January and 13 July stain lines. The dashed vertical lines mark the end of the upwelling season each year according to the SST record. In 2003, the dashed line also corresponds to the 15 April stain line.

Table 5
Average coral skeletal Cd concentrations obtained by laser ablation (LA) inductively coupled plasma mass spectrometry (ICP-MS) (LA-$[Cd]_{coral}$) and isotope dilution (ID-$[Cd]_{coral}$).

	LA-$[Cd]_{coral}$ (ng g^{-1})		ID-$[Cd]_{coral}$ (ng g^{-1})	
	Upwelling	Non-Upwelling	Upwelling	Non-upwelling
Porites lobata	28.0	23.9	3.4[a]	2.4[a]
Pavona gigantea	27.0	21.5	22.8[a]	11.4[a]
Pavona clavus	26.9	23.8	23.1[a]	8.7[a]
			24.0	19.0

[a] Bulk values from Matthews et al. (2008).

of Cd into both the tissue and the skeleton. Alternatively, staining experiments have revealed that up to 50% of total calcification occurs in the weeks to months after initial deposit of the skeletal structure (Barnes and Lough, 1993; Taylor et al., 1993). This secondary skeletal backfilling implies that some of the skeleton deposited during peak $[Cd]_{sw}$ was layered over older, previously precipitated skeleton, which could lead to an apparent offset between the peak coral and seawater Cd values.

Irrespective of which mechanism(s) underlies the 1-month offset in coral and seawater Cd values, as long as it is consistent over time, the offset can be taken into account when reconstructing $[Cd]_{sw}$ from $[Cd]_{coral}$ as shown in Eqs. (3) and (4). However, the calibration equations generated here may only apply to corals from sites where the biological and chemical dynamics are similar to those in the upwelling regions of the Gulf of Panama. While these results are encouraging, additional measurements in additional colonies are needed to validate these calibration equations for *P. clavus* and further detailed study is needed to establish calibration equations for other species.

4.4. A 3-year skeletal LA-$[Cd]_{coral}$ record

The 3-year *P. clavus* $[Cd]_{coral}$ record had three salient features: 1) three distinct annual $[Cd]_{coral}$ cycles, 2) a large $[Cd]_{coral}$ enrichment in 2003, and 3) maximum $[Cd]_{coral}$ lagged minimum SST and maximum Chl *a* by ~1 month (Fig. 6). While the timing of the annual $[Cd]_{coral}$ peaks was similar each year, the magnitude of the $[Cd]_{coral}$ enrichment was much greater in 2003 than in the other two years (Fig. 6C). The high $[Cd]_{coral}$ during 2003 did not appear to be the result of a particularly strong upwelling season as indicated by Chl a or SST. However, local SST values indicate that the local upwelling may have been stronger than what was detected at the regional scale with the satellite SST data (Fig. 6A). Another possibility could be related to tissue contamination. Although coral Cd has been long thought to occur as a substitution for Ca^{+2} in the mineral lattice, incomplete cleaning (e.g., cleaning coral slabs for LA analysis where not all surfaces are exposed) may lead to elevated $[Cd]_{coral}$, particularly in near-tissue areas because tissue is known to be enriched in Cd by a factor of ~100 (Esslemont, 2000; Esslemont et al., 2000). However, the large 2003 enrichment in the multi-year record occurred well below the tissue layer and is therefore more likely due to higher local $[Cd]_{sw}$, irrespective of regional SST or Chl *a* values.

The offset between peak $[Cd]_{coral}$ and minimum SST and peak Chl *a* in 2001 and 2002 (Fig. 6) was expected given the observed offset between SST and $[Cd]_{coral}$ in 2003 (Figs. 4 & 6).

Additional studies on the same coral fragments have shown that coral skeletal phosphorus to calcium ratios (P/Ca) measured by LA-ICP-MS is directly correlated with seawater phosphate concentrations and that both seawater concentrations and coral P/Ca values peaked in mid-March of 2003 (LaVigne et al., 2010) — coinciding with the timing of $[Cd]_{coral}$ in this study. Thus, Chl *a* and SST lead both $[Cd]_{coral}$ and coral skeletal P/Ca by ~1 month and $[Cd]_{sw}$ by ~2 months. The exact timing of both the coral skeletal Cd and P/Ca peaks indicates that both are being taken up by corals at the same time, but does not allow us to determine if Cd is being taken up by corals as a micronutrient (i.e. Morel and Price, 2003; Cullen and Maldonado, 2013) or as a toxin that is acquired as a consequence of other nutrient uptake (Horner et al., 2013). In addition, our data do not allow us to determine how the corals take up the Cd, but viable mechanisms could include one or more of the following: heterotrophic feeding (i.e., ingestion of phytoplankton, zooplankton, dissolved and particulate organic matter), uptake of the dissolved inorganic Cd by the endosymbiotic algae, and direct incorporation of inorganic Cd into the skeleton from seawater. Further research would be needed to fully tease out the proportionate contribution of each source of Cd to the coral skeleton.

Irrespective of the reason for Cd uptake and incorporation into coral skeletons, the predictable relationship between coral and seawater [Cd] allows us to reconstruct past $[Cd]_{sw}$ concentrations from $[Cd]_{coral}$ in the Gulf of Panama. The predicted $[Cd]_{sw}$ values generated using Eq. (3) do illustrate the expected lag in Cd accumulation in the seawater during upwelling events (Fig. 6C) and offer encouragement that $[Cd]_{sw}$ reconstructions can be generated from $[Cd]_{coral}$ records. Similar lags between SST and coral skeletal Ba/Ca at upwelling sites have also been reported (Tudhope et al., 1996; Ourbak et al., 2006). This reinforces the argument that early cold-water upwelling pulses of $[Cd]_{sw}$ are rapidly taken up by phytoplankton, then coral, and only then accumulate in the water column once the biota is no longer Cd-limited as suggested by the predicted $[Cd]_{sw}$ values.

The observed offsets between peak $[Cd]_{coral}$ and minimum SST, peak Chl a, and peak $[Cd]_{sw}$ (Figs. 4 & 6) are an important feature that not only affect our understanding of upwelling dynamics, but have implications for multi-proxy paleoclimate reconstruction. For example we propose that coral skeletal $\delta^{18}O$-based temperature proxy records should not be forced to line up exactly with $[Cd]_{coral}$ when "squiggle-matching", but should be offset by a month. Finally, while this single 3-year $[Cd]_{coral}$ is very encouraging, it is based on only a single coral. Given the high natural variability of LA-derived $[Cd]_{coral}$ within colonies (Fig. 2) and variability among colonies of the same species (Matthews et al., 2008), at least three laser tracks per colony and three colonies per species are recommended for producing a robust environmental history. This recommendation is similar to the coral core "stacking" approach suggested by Lough (2004).

Acknowledgments

The authors thank R. Ash, O. Gibb, L. D'Croz, L. Rodrigues, and R. Moyer and the Smithsonian Tropical Research Institute. Funding was provided to K.A.M. from the Evolving Earth Foundation and to J.E.P. by the Government of Alberta Sir James Lougheed Award of Distinction. The majority of the funding was provided to A.G.G. by the Petroleum Research Foundation (No. 41740-G2) and the National Science Foundation program in Chemical Oceanography (OCE No. 0610487). K.A.M. and J.E.P. were students of A.G.G.'s.

References

Achterberg, E., Ryan, C., Jackson, S., Griffin, W., 2001. Appendix 3: data reduction software for LA-ICP-MS. In: Sylvester, P. (Ed.), Laser Ablation-ICP-MS in the Earth Sciences. Mineralogical Associate of Canada, p. 243.

Alibert, C., et al., 2003. Source of trace element variability in Great Barrier Reef corals affected by the Burdekin flood plumes. Geochim. Cosmochim. Acta 67 (2), 231–246.

Allison, N., Finch, A.A., 2004. High-resolution Sr/Ca records in modern *Porites lobata* corals: effects of skeletal extension rate and architecture. Geochem. Geophys. Geosyst. 5 (5). http://dx.doi.org/10.1029/2004GC000696.

Barnes, D.J., Lough, J.M., 1993. On the nature and causes of density banding in massive coral skeletons. J. Exp. Mar. Biol. Ecol. 167, 91–108.

Carriquiry, J., Villaescusa, 2010. Coral Cd/Ca and Mn/Ca records of ENSO variability in the Gulf of California. Clim. Past 6, 401–410.

Chen, L., et al., 2011. Accurate determinations of fifty-four major and trace elements in carbonate by LA-ICP-MS using normalization strategy of bulk components as 100%. Chem. Geol. 284, 283–295.

Craig, C.A., Jarvis, K.E., Clarke, L.J., 2000. An assessment of calibration strategies for the quantitative and semi-quantitative analysis of calcium carbonate matrices by laser ablation-inductively coupled plasma-mass spectrometry (LA-ICP-MS). J. Anal. At. Spectrom. 15 (8), 1001–1008.

Cullen, J.T., Maldonado, M.T., 2013. Biogeochemistry of cadmium and its release to the environment. In: Sigel, A., Sigel, H., Sigel, R.K.O. (Eds.), Cadmium: From Toxicity to Essentiality. Springer, pp. 31–58.

D'Croz, L., Robertson, D.R., 1997. Coastal oceanographic conditions affecting coral reefs on both sides of the isthmus of Panama. Proceedings of the 8th International Coral Reef Symposium, 2, pp. 2053–2058.

D'Croz, L., del Rosario, J.B., Gomez, J.A., 1991. Upwelling and phytoplankton in the Bay of Panamá. Rev. Biol. Trop. 39 (2), 233–241.

Delaney, M.L., Linn, L.J., Druffel, E.R.M., 1993. Seasonal cycles of manganese and cadmium in coral from the Galapagos Islands. Geochim. Cosmochim. Acta 57 (1), 347–354.

Dunbar, R.G., Wellington, G.M., Colgan, M.W., Glynn, P.W., 1994. Eastern Pacific sea surface temperature since 1600 A.D.: the δ^{18}O record of climate variability in Galapagos corals. Paleoceanography 9 (2), 291–315.

Eakin, C.M., Grottoli, A.G., 2006. Paleo-climate changes and corals. In: Phinney, J., Skirving, W., Kleypas, J., Hoegh-Guldberg, O., Strong, A.E. (Eds.), Coral Reefs and Climate Change: Science and Management. Coastal and Estuarine Studies, 61, pp. 33–54.

Esslemont, G., 2000. Heavy metals in seawater, marine sediments and corals from the Townsville section, Great Barrier Reef Marine Park, Queensland. Mar. Chem. 71, 215–231.

Esslemont, G., Harriott, V.J., McConchie, D.M., 2000. Variability of trace-metal concentrations within and between colonies of *Pocillopora damicornis*. Mar. Pollut. Bull. 40 (7), 637–642.

Fallon, S.J., McCulloch, M.T., van Woesik, R., Sinclair, D.J., 1999. Corals at their latitudinal limits: laser ablation trace element systematics in Porites from Shirigai Bay, Japan. Earth Planet. Sci. Lett. 172, 221–238.

Fallon, S.J., White, J.C., McCulloch, M.T., 2002. *Porites* corals as recorders of mining and environmental impacts: Misima Island, Papua New Guinea. Geochim. Cosmochim. Acta 66, 45–62.

Fallon, S.J., McCulloch, M.T., Alibert, C., 2003. Examining water temperature proxies in Porites corals from the Great Barrier Reef: a cross-shelf comparison. Coral Reefs 22 (4), 389–404.

Field, M., Cullen, J., Sherrell, R., 1999. Direct determination of 10 trace metals in 50 μL samples of coastal seawater using desolvating micronebulization sector field ICP-MS. J. Anal. At. Spectrom. 14, 1425–1432.

Glynn, P.W., Ault, J.S., 2000. A biogeographic analysis and review of the far eastern Pacific coral reef region. Coral Reefs 19, 1–23.

Glynn, P.W., Mate, J.L., 1997. Field guide to the Pacific coral reefs of Panama. Proceedings of the 8th International Coral Reef Symposium, 1, pp. 145–166.

Grottoli, A.G., Eakin, C.M., 2007. A review of modern coral δ^{18}O and Δ^{14}C proxy records. Earth Sci. Rev. 81, 67–91.

Grottoli, A.G., Rodrigues, L.J., Palardy, J.E., 2006. Heterotrophic plasticity and resilience in bleached corals. Nature 440 (7088), 1186–1189.

Hart, S.R., Cohen, A.L., 1996. An ion probe study of annual cycles of Sr/Ca and other trace elements in corals. Geochim. Cosmochim. Acta 60, 3075–3084.

Horibe, Y., Endo, K., Tsubota, H., 1974. Calcium in the South Pacific and its correlation with carbonate alkalinity. Earth Planet. Sci. Lett. 23, 136–140.

Horner, T.J., Lee, R.B.Y., Henderson, G.M., Rickaby, R.E.M., 2013. Nonspecific uptake and homeostasis drive the oceanic cadmium cycle. Proc. Natl. Acad. Sci. U. S. A. 110 (1), 2500–2505.

Kroslakova, I., Gunther, D., 2007. Elemental fractionation in laser ablation-inductively coupled plasma-mass spectrometry: evidence for mass load induced matrix effects in the ICP during ablation of a silicate glass. J. Anal. At. Spectrom. 22, 51–62.

LaVigne, M., et al., 2010. Coral skeleton P/Ca proxy for seawater phosphate: multi-colony calibration with a contemporaneous seawater phosphate record. Geochim. Cosmochim. Acta 74 (4), 1282–1293.

Lea, D.W., Shen, G.T., Boyle, E.A., 1989. Coralline barium records temporal variability in equatorial Pacific upwelling. Nature 340, 373–376.

Legendre, P., 2011. lmodel2: Model II Regression, R Package Version 1.7-0.

Legendre, P., Legendre, L., 1998. Numerical Ecology. Elsevier, Amsterdam (853 pp.).

Linn, L.J., Delaney, M.L., Druffel, E.R.M., 1990. Trace metals in contemporary and seventeenth-century Galapagos coral: records of seasonal and annual variations. Geochim. Cosmochim. Acta 54, 387–394.

Lough, J.M., 2004. A strategy to improve the contribution of coral data to high-resolution paleoclimatology. Palaeogeogr. Palaeoclimatol. Palaeoecol. 204, 115–143.

Matthews, K.A., McDonough, W.F., Grottoli, A.G., 2006. Cadmium measurements in coral skeleton using isotope dilution-inductively coupled plasma-mass spectrometry. Geochem. Geophys. Geosyst. 7.

Matthews, K.A., Grottoli, A.G., McDonough, W.F., Palardy, J.E., 2008. Upwelling, species, and depth effects on coral skeletal cadmium-to-calcium ratios (Cd/Ca). Geochim. Cosmochim. Acta 72 (18), 4537–4550.

McConnaughey, T., 1989. ^{13}C and ^{18}O isotopic disequilibrium in biological carbonates: I. Patterns. Geochim. Cosmochim. Acta 53, 151–162.

McCulloch, M., et al., 2003. Coral record of increased sediment flux to the inner Great Barrier Reef since European settlement. Nature 421 (6924), 727–730.

Morel, F.M.M., Price, N.M., 2003. The biogeochemical cycles of trace metals in the oceans. Science 300, 944–947.

Ourbak, T., et al., 2006. A high-resolution investigation of temperature, salinity, and upwelling activity proxies in corals. Geochem. Geophys. Geosyst. 7 (3), 1–13.

Palardy, J.E., Grottoli, A.G., Matthews, K.A., 2005. Effects of upwelling, depth, morphology and polyp size on feeding in three species of Panamanian corals. Mar. Ecol. Prog. Ser. 300, 79–89.

Palardy, J.E., Grottoli, A.G., Matthews, K.A., 2006. Effect of zooplankton abundance on natural feeding rates of two coral species in the eastern Pacific. J. Exp. Mar. Biol. Ecol. 331, 99–107.

Palardy, J.E., Rodrigues, L.J., Grottoli, A.G., 2008. The importance of zooplankton to the daily metabolic carbon requirements of healthy and bleached corals at two depths. J. Exp. Mar. Biol. Ecol. 367 (2), 180–188.

Pearce, N., et al., 1997. A compilation of new and published major and trace element data for NIST SRM 610 and NIST SRM 612 glass reference materials. Geostand. Newslett. 21 (1), 115–144.

Reuer, M.K., Boyle, E.A., Cole, J.E., 2003. A mid-twentieth century reduction in tropical upwelling inferred from coralline trace element proxies. Earth Planet. Sci. Lett. 210, 437–452.

Reynolds, R., Smith, T., 1994. Improved global sea surface temperature analyses. J. Clim. 7, 929–948.

Shen, G.T., Sanford, C.L., 1990. Trace element indicators of climate variability in reef-building corals. In: Glynn, P.W. (Ed.), Global Ecological Consequences of the 1982–83 El Niño-Southern Oscillation. Elsevier, New York, pp. 255–283.

Shen, G.T., Boyle, E.A., Lea, D.W., 1987. Cadmium in corals as a tracer of historical upwelling and industrial fallout. Nature 328 (6133), 794–796.

Shen, G.T., et al., 1992. Surface ocean variability at Galapagos from 1936–1982: calibration of geochemical tracers in corals. Paleoceanography 7 (5), 563–588.

Sinclair, D., 2005a. Non-river flood barium signals in the skeletons of corals from coastal Queensland, Australia. Earth Planet. Sci. Lett. 237, 354–369.

Sinclair, D.J., 2005b. Correlated trace element “vital effects” in tropical corals: a new geochemical tool for probing biomineralization. Geochim. Cosmochim. Acta 69 (13), 3265–3284.

Sinclair, D.J., Kinsley, L.P.J., McCulloch, M.T., 1998. High resolution analysis of trace elements in corals by laser ablation ICP-MS. Geochim. Cosmochim. Acta 62 (11), 1889–1901.

Stephans, C.L., Quinn, T.M., Taylor, F.W., Corrège, T., 2004. Assessing the reproducibility of coral-based climate records. Geophys. Res. Lett. 31. http://dx.doi.org/10.1029/2004GL020343.

Taylor, R.B., Barnes, D.J., Lough, J.M., 1993. Simple models of density band formation in massive corals. J. Exp. Mar. Biol. Ecol. 167, 109–125.

Tudhope, A.W., Lea, D.W., Shimmield, G.B., Chilcott, C.P., Head, S., 1996. Monsoon climate and Arabian Sea coastal upwelling recorded in massive corals from southern Oman. Palaios 11, 347–361.

Wellington, G.M., Dunbar, R.B., 1995. Stable isotopic signature of El Nino-Southern Oscillation events in eastern tropical Pacific reef corals. Coral Reefs 14, 5–25.

Wyndham, T., McCulloch, M., Fallon, S., Alibert, C., 2004. High-resolution coral records of rare earth elements in coastal seawater: biogeochemical cycling and a new environmental proxy. Geochim. Cosmochim. Acta 68, 2067–2080.